Available online at www.sciencedirect.com
ScienceDirect
Chemical Physics Letters 430 (2006) 330–335
CHEMICAL PHYSICS LETTERS
www.elsevier.com/locate/cplett

Morphology and optical properties of MgO thin films on Mo(001)

S. Benedetti [a], H.M. Benia [b], N. Nilius [b,*], S. Valeri [a], H.J. Freund [b]

[a] *Dipartimento di Fisica, Università di Modena e Reggio Emilia and CNR-INFM National Research Center on nanoStructures and bioSystems at Surfaces (S3), Via G. Campi 213/a, 41100 Modena, Italy*
[b] *Fritz-Haber-Institut der Max-Planck-Gesellschaft, Faradayweg 4-6, D-14195 Berlin, Germany*

Received 21 July 2006; in final form 25 August 2006
Available online 5 September 2006

Abstract

Thin MgO films with a nominal thickness ranging between 1 and 60 ML have been grown on a Mo(001) surface. The film morphology was studied by LEED and STM, revealing the presence of a coincidence pattern with the Mo support in the low coverage regime, a dislocation network at medium thickness and a rather flat and defect-poor MgO surface for thicker layers. The MgO optical properties were investigated as a function of film thickness by analyzing electro-luminescence spectra obtained via electron injection from the STM tip into well-defined surface areas. The spectra are characterized by two distinct emission bands at 3.1 and 4.4 eV. Their origin is discussed in the light of earlier photo-luminescence measurements on MgO nanocubes and smokes.

1. Introduction

Insulating metal oxides have attracted wide interest in recent years due to their potential applications as support for metal nano-particles in electronic devices, heterogeneous catalysts and gas sensing systems [1,2]. In particular, they are often used in the form of thin films, because of novel properties arising from interactions with the metal substrate and the possibility to investigate such systems with surface science methods based on electrons or ions, in spite of their insulating character.

Among these materials, MgO is especially promising thanks to its wide bandgap and the good chemical [3] and thermal stability [4]. The compound is easy to prepare due to the high oxygen affinity and low melting temperature of Mg. The simple rock-salt structure allows the growth of epitaxial films on a variety of substrates, as long as the lattice mismatch with the MgO does not exceed 5–7%. Stoichiometry, structure and morphology have been intensively investigated for MgO deposited on Ag(001) [5–9], Fe(001) [10,11] and Mo(001) [4,12–14]. Particularly interesting is the use of Mo supports, because of the possibility to treat the films at high temperatures. High temperature deposition or post-growth annealing, which is not applicable for Ag and Fe substrates, is usually performed to improve the film morphology and reduce its defectiveness. In spite of these advantages, the morphology of the MgO/Mo system has not been extensively investigated in the past. The only work [14] published so far shows that the surface changes dramatically for a MgO deposition temperature above 1100 K, whereas deposition at 300 K followed by post-annealing does not improve the film morphology.

The physical and chemical properties of oxide surfaces are often dominated by the presence of defects, which might occur in the form of vacancies and low-coordinated sites. While bulk MgO, for example, does not absorb nor emit light in the range between 200 and 900 nm, pronounced luminescence bands have been observed for MgO smokes [15–17] and powders [18,19] at energies much lower than the bulk bandgap. These emission bands have been assigned to the presence of low-coordinated sites and colour centres at the surface; however, no consensus is reached so far on their relative contribution to the photon signal. In addition, the adsorption of molecules and atoms has been traced back to the abundance of defects in the MgO surface, emphasizing their important role for

* Corresponding author. Fax: +49 30 8413 4101.
E-mail address: nilius@fhi-berlin.mpg.de (N. Nilius).

0009-2614/$ - see front matter © 2006 Elsevier B.V. All rights reserved.
doi:10.1016/j.cplett.2006.08.130

the nucleation behaviour and the catalytic properties of this oxide material.

This Letter aims to provide new information on the interplay between the morphology of MgO thin films and their optical properties. For this purpose, MgO films of varying thickness have been prepared on Mo(001) and studied by means of LEED, scanning tunnelling microscopy (STM) and luminescence spectroscopy induced by field-emitted electrons from the STM tip [20]. These methods give complementary information on the topographic and optical properties of MgO thin films.

2. Experimental

Experiments are carried out with a beetle-type STM operated at liquid-nitrogen temperature (100 K) and ultra-high vacuum conditions ($p \sim 5 \times 10^{-10}$ mbar) [20]. A parabolic mirror surrounding the microscope head collects photons emitted from the tunnel junction. A second mirror outside the vacuum chamber focuses the light onto the entrance slit of a grating spectrograph attached to a liquid-nitrogen cooled CCD detector. A LEED system enables easy control of the sample quality after preparation. The Mo(001) single crystal is prepared by repeated cycles of annealing at 1300 K in O_2 atmosphere and flashes to 2300 K in UHV. This produces a sharp $p(1 \times 1)$ LEED pattern and a surface with large terraces (>200 nm) delimited by monatomic steps. The MgO film is grown by reactive deposition of Mg in an O_2 partial pressure of 1×10^{-7} mbar with the Mo substrate held at room temperature. Magnesium is evaporated from a crucible heated by electron bombardment. After deposition, the sample is annealed for 10 min at 1100 K to improve the crystallinity of the film. For sub-monolayer films, the MgO coverage is directly deduced from STM images, whereas for thicker films, a nominal thickness is defined as product between MgO deposition rate and exposure time.

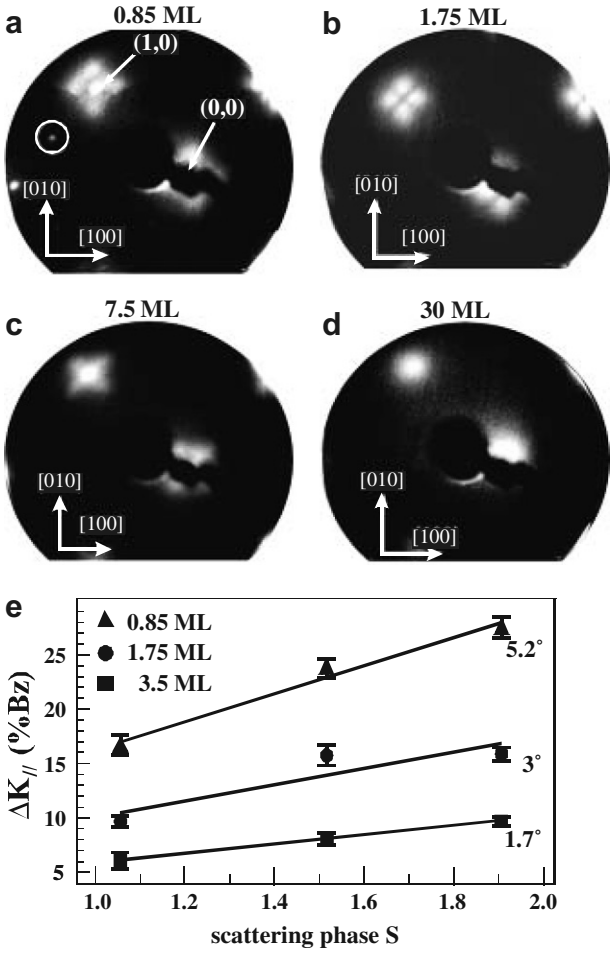

Fig. 1. LEED pattern of MgO films on Mo(001): (a) 0.85 ML, (b) 1.75 ML, (c) 7 ML and (d) 30 ML ($E_p = 55$ eV). The circle in (a) marks one of the (2×2) superstructure spots. (e) Positions of [100] satellites with respect to the central spot in the Brillouin zone shown as a function of the scattering phase $S = dK_\perp/2\pi$ [21]. The lines are linear fits to the data and yield information on the tilting angles with respect to the ideal (001) surface.

3. Results

Fig. 1 shows a series of LEED patterns of MgO films with increasing thickness. In all cases, a square (1×1) structure is observed. From the identical size of the primitive cell on the clean substrate and the film, epitaxial growth of the oxide on Mo(001) is concluded. Hereby, the MgO(001) plane is parallel to Mo(001) while the MgO[100] direction aligns with the Mo[110] direction, as expected from the 5% lattice mismatch between the primitive cells of bcc Mo (3.15 Å) and rock-salt MgO (2.98 Å). For sake of clarity, all crystallographic directions in this Letter are given with respect to the MgO. The appearance of a $p(2 \times 2)$ superstructure in the low-coverage regime (Fig. 1a) is attributed to the formation of a Mg–Mo–O interface layer. Evidence for such alloying effect is gained from STM and optical measurements and will be presented in a forthcoming paper. The fundamental spots in low-thickness preparations show an anisotropic broadening, which evolves to clear and distinct satellites oriented along the MgO[100] at 2–5 ML nominal thickness (Fig. 1a). Depending on the primary electron energy, the central spot of each fundamental reflex appears and disappears in this growth stage and additional satellites become visible along the [110] direction (not shown here). We attribute this behaviour to interference effects between neighbouring MgO domains in antiphase scattering configuration. With increasing film thickness, the [100] satellite spots move towards the central spot and finally disappear at around 5 ML thickness (Fig. 1b). The splitting of fundamental reflexes with respect to the first Brillouin zone depends linearly on the primary electron energy, as shown in Fig. 1e. This observation is compatible with a Moiré structure comprising tilted MgO facets, in agreement with the STM results discussed below. For a nominal thickness between 5 and 12 ML, distinct crosses appear in the LEED pattern around each fundamental spot oriented along the [110] direction (Fig. 1c). Similar observations were reported ear-

lier for MgO/Ag(100) [21] and MgO/Fe(100) [22] and assigned to the formation of mosaics spanned between a dislocation network that relaxes the strain in the oxide layer. The size of the [110] crosses in LEED is directly connected to the inclination angle of the tilted regions and decreases with increasing thickness. Finally, for films consisting of more than 15 layers a simple (1×1) pattern appears in LEED, indicating a flat and defect-poor surface structure (Fig. 1d).

The evolution of the MgO morphology with increasing film thickness is also analysed by STM as summarized in Fig. 2. After deposition of approximately one layer, the film still exhibits large holes, confined by non-polar [100] and polar [110] oriented edges (Fig. 2a). The presence of a significant fraction of polar borders has already been observed for thin MgO films on Ag(100) and ascribed to a stabilization effect of the metal support [23]. On the oxide surface, a regular square pattern with a mean size of 55 Å becomes visible, which is aligned with the MgO [110] direction. The pattern persists until 5 ML nominal film thickness, which corresponds to the range where [100] satellite spots are present in LEED. The square structure is interpreted as coincidence lattice resulting from the 5% lattice mismatch between MgO and Mo and would be compatible with 18 MgO unit cells overlaying 17 substrate cells along the MgO[110] direction. The calculated size of such Moiré structure amounts to 53.5 Å, in good correspondence to the periodicity of the measured square pattern. The visibility of the Moiré structure is apparently enhanced by an electronic effect, as large topographic contrast is only obtained for sample voltages above 3.5 V [24]. The occurrence of four satellite spots around each fundamental LEED reflex suggests furthermore that each Moiré unit cell consists of four regions tilted along the MgO⟨100⟩ directions. From the change of the relative position of the LEED satellites in the first Brillouin zone as a function of energy, a maximum tilting angle of 5° with respect to MgO(001) is concluded for ultra-thin films, which rapidly reduces to zero with increasing film thickness (Fig. 1e).

The surface Moiré pattern fades away for a nominal MgO thickness of 3–5 ML. The dominant structural elements on the surface are now step edges, dislocation lines and small rectangular holes of 20–50 Å diameter (Fig. 2b). Whereas for thinner films, dislocation lines have no preferential orientation, they begin to align with the MgO[100] direction for thicker ones. In particular cases, the presence of screw dislocations can be recognized, as shown in the inset of Fig. 2c. The formation of a dislocation network is a well-known mechanism to reduce stress and strain in thin epitaxial films caused by a lattice mismatch with the support [25]. The presence of a dislocation network at this growth stage is also reflected by the characteristic crosses around each fundamental spot in the LEED measurements (Fig. 1c). Above 7 ML film thickness, the oxide gradually flattens and the global roughness decreases, indicating good layer-by-layer growth. This

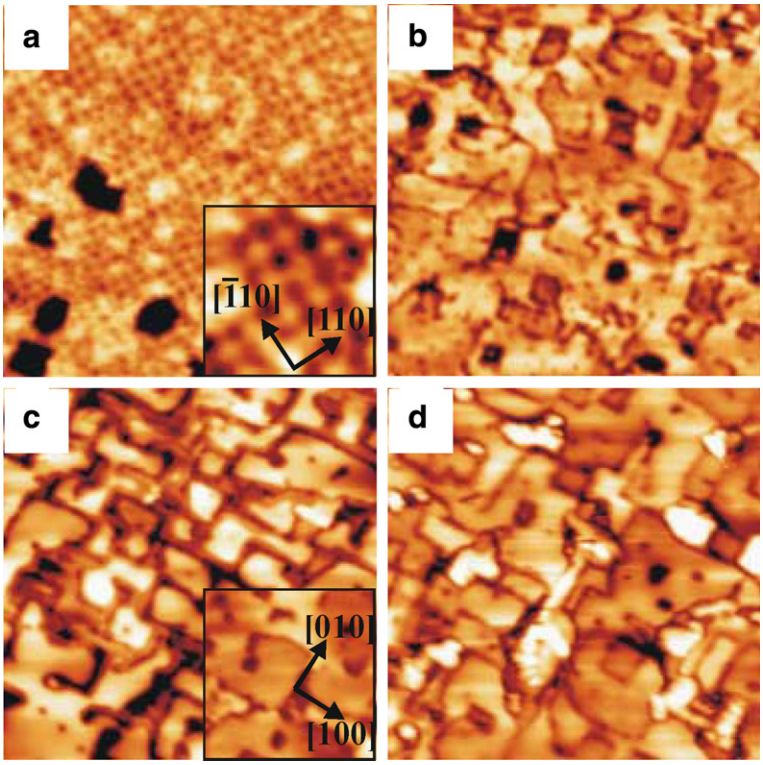

Fig. 2. STM images of MgO thin films on Mo(001): (a) 150×150 nm^2 of 0.85 ML MgO ($I=0.23$ nA, $U_{\text{Sample}}=+3.4$ V). The inset shows a 25×25 nm^2 region of the same sample. (b) 1.75 ML MgO ($I=0.05$ nA, $U_{\text{Sample}}=+3$ V), (c) 7 ML MgO ($I=0.14$ nA, $U_{\text{Sample}}=+3.7$ V); (d) 18 ML ($I=0.15$ nA, $U_{\text{Sample}}=+12.5$ V). Images (b–d) are 100×100 nm^2 in size. The inset in image c shows a screw dislocation, which is frequently observed in 5–10 ML thick MgO films.

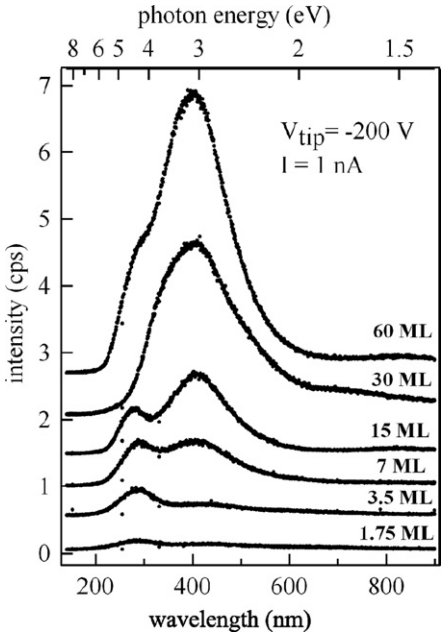

Fig. 3. Photon emission spectra collected from MgO films with increasing thickness. Excitation conditions were kept constant in all spectra (electron energy: −200 eV, current: 1 nA, acquisition time: 60 s).

trend finds its correspondence in the LEED pattern, where the complex spot structure transforms into single (1×1) LEED spots. For a nominal thickness exceeding 15 ML, STM experiments become increasingly difficult due to the vanishing conductivity of the film and only step edges remain visible at the surface (Fig. 2d).

To correlate the structural properties described above with optical parameters, luminescence measurements are performed on thin MgO films grown on Mo(0 0 1). The photon emission is excited via electron injection from the STM tip into well-characterized surface areas imaged prior to spectroscopic measurements. Emission spectra are acquired for electron energies ranging between 50 and 200 eV; whereby current and acquisition time are limited to 1 nA and 60 s, respectively, to reduce electron-induced damage of the film. With increasing electron energy, an exponential increase of the photon yield is observed; however, the spectral characteristic of the emission remains unchanged. Fig. 3 presents a series of photon emission spectra taken at −200 V tip bias for MgO films containing up to 60 layers. Spectra excited with lower electron energies (50 eV) are qualitatively similar, but show reasonable signal to noise ratios only for extended accumulation times. In all spectra, two emission bands are identified, located around 280 nm (4.4 eV) and 400 nm (3.1 eV), respectively.[1] With increasing film thickness, both bands gain intensity, whereby the low-energy band at 3.1 eV is more affected. Saturation of the total emission yield is observed for films thicker than 40 ML. As geometric and electronic tip properties slightly vary with time, the experimental set-up does not allow for a quantitative comparison of the emitted light intensity.

In the literature, the characteristic light emission from MgO surfaces is rationalized by the following mechanism. In a first step, surface excitons are formed by interactions of O^{2-} ions with photons or electrons. They are dominantly excited at 5-fold coordinated terrace sites (5C sites), simply because they represent the most abundant surface site. Excitonic modes on the MgO surface are mobile and can move away from their excitation centre in a random-walk type process [26]. The diffusion stops when the electron–hole pair becomes trapped at defect sites (e.g. F centres) or sites with lower local coordination, such as 4-fold coordinated edge (4C) or 3-fold coordinated corner sites (3C). The trapping occurs because of the smaller Madelung potential at low-coordinated sites, resulting in a stabilization of the electron–hole pair [26]. Defects and low-coordinated edge or corner sites are therefore preferential recombination centres for surface excitons and dominate the emission characteristics of MgO. The relative importance of the two exciton-decay pathways, either via corner and edge sites or via oxygen vacancies, is heavily debated in the literature. In recent photo-luminescence measurements on defect-poor MgO nanocubes, two emission bands have been identified at 3.84 eV and 3.2 eV and assigned to the radiative recombination of excitons at 4C edge and 3C corner sites, respectively [15,17]. This interpretation is in accordance to previous data on MgO smokes [18] and theoretical calculations [26,27]. Slightly different results were reported by other groups, with emission bands somewhat red-shifted to 3.2 eV for the 4C and 2.7 eV for the 3C emission centres [16,19]. On the other hand, an emission band at 3.2 eV detected for MgO single crystals was claimed to originate from an emission mechanism involving F^+ centres [28].

To discriminate between the two proposed mechanisms, colour centres have been intentionally introduced into the surface by exposing the MgO film to a flux (1 mA) of 300 eV electrons for 10 min prior to spectroscopy. Electron bombardment induces desorption of O atoms from the MgO surface in an Auger-like process, and should thus intensify the emission channel involving colour centres [29]. However, decreasing emission intensity was observed for electron-bombarded films, pointing towards a minor role of surface colour centres in the emission process (Fig. 4a). The reverse approach, namely annihilation of potential colour centres by healing MgO films in 1×10^{-7} mbar oxygen, led to a similar conclusion, as the emission yield was not completely quenched even after prolonged O_2 exposure (Fig. 4a).

For the interpretation of the optical data, the electron exposure during spectral acquisition has to be considered, too. In a typical spectrum taken with 1 nA field-emission

[1] Bremsstrahlung created by the injection of high-energy electrons into the sample has to be taken into account as additional source of UV photon emission. Due to the wavelength cut-off of the CCD detector, this produces an artificial emission maximum around 250–270 nm that might contribute to the 280 nm band. The effect is stronger for thin MgO layers, because Bremsstrahlung is more effectively produced by electron injection into the underlying metal support.

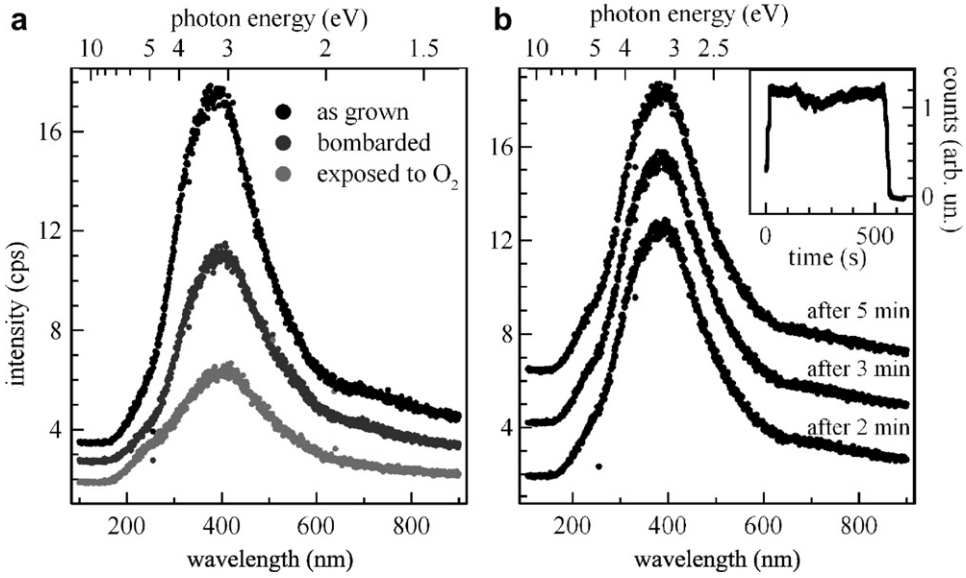

Fig. 4. (a) Photon emission spectra from a 30 ML thick MgO film. Upper curve: as prepared film, central curve: after electron bombardment (300 eV, 10 min) and lower curve: after exposure to 45 Langmuir O_2. Neither changes in the spectral shape nor variation in intensity are observed that would be compatible with a dominant role of surface colour centres. (b) Series of photon emission spectra from a 30 ML thick MgO film on Mo(001) (electron energy: −240 V, current: 1 nA, acquisition time: 60 s). Numbers next to each curve indicate the total electron exposure time the surface has experienced during spectroscopy. The inset shows the time evolution of the total emission intensity during spectral acquisition from a freshly prepared MgO film detected with a photomultiplier. After reaching the maximum, the photon intensity remains relatively constant over the full acquisition time of 10 min. See text for details.

current from the STM tip, approximately 100 electrons per second are injected into every anion site. This dosage is sufficient to induce a reasonable quantity of surface colour centres, provided that the electron energy exceeds the threshold for electron-induced O-desorption. Two observations suggest that colour centres formed during spectral acquisition are not the main cause of the light emission. First, spectra exhibiting the distinct emission bands at 3.1 and 4.4 eV are obtained even for excitation energies below 50 eV, where electron-induced colour centre formation is inefficient [21]. Second, photon yield as well as spectral characteristics of the MgO emission was found to be constant over several minutes of data acquisition (Fig. 4b), although the number of O vacancies and therewith the emission yield should continuously rise with acquisition time. In combination with results on intentionally electron-bombarded versus oxygen-treated films, colour centres have thus been ruled out as the dominant source of light emission from the MgO surface.

The two bands in our optical emission spectra are therefore interpreted as signature of radiative exciton decays from low-coordinated MgO sites. The emission peak at 3.1 eV agrees well with the main feature detected in previous photo-luminescence experiments on cube-shaped MgO nanocrystals [15,16]. Based on model calculations, this band has been assigned to emission centres located at 3C corner sites on the MgO surface [26]. The energy of the second peak (4.4 eV) in our experiment indicates an emission pathway involving higher coordinated sites. Similar bands in photo-luminescence spectra have been attributed to emission from 4C anion sites located at MgO step edges [15]. An unambiguous assignment of the 4.4 eV peak is not possible here due to the less-regular film morphology compared to well-defined MgO nanocubes. Beside step edges, other low-coordinated sites might be relevant for optical transitions above 4.0 eV in the MgO/Mo(001) system, such as kinks, irregular and inverse corners.[2]

Our interpretation of the light emission as radiative decay of MgO excitons trapped at low-coordinated sites also provides an explanation for the observed dependence of the emission yield on the film thickness. The probability for a surface exciton to reach a low-coordinated step or corner after excitation on a distant terrace site depends on the lifetime of the electron–hole pair and the surface morphology. In the case of ultra-thin MgO films on Mo(001), the exciton lifetime is governed by the presence of non-radiative decay channels provided by the metal support (Landau damping). The exciton lifetime and therefore its probability to undergo a radiative recombination increase when the MgO surface is spatially decoupled from the Mo substrate via a thick oxide layer. This behaviour is reflected in our experimental finding that the emission yield initially increases with film thickness, but saturates for

[2] MgO luminescence peaks observed in our experiment are generally red-shifted with respect to earlier photo-luminescence data. A number of reasons might be responsible for this discrepancy. First, the MgO film has only limited thickness and is supported by a Mo(001) crystal. Interactions between electron–hole pair excitations in the oxide and their image in the highly polarizable metal support lead to smaller excitation energies. Second, the presence of a biased tip in close proximity to the sample surface produces a strong electric field in the oxide film that shifts optical transition energies via the Stark effect.

higher MgO coverage. The influence of the metal vanishes for films containing more than 40 layers, which enables a rough estimation of the interaction length between MgO surface excitons and electronic excitations in the Mo support.

Finally, we want to emphasize that structural changes in the MgO surface during electron injection from the STM tip cannot be excluded. Radiation- and electron-induced damage on oxide and halogenide surfaces is described in the literature in great detail [30–32]. Usually, the emergence of holes is observed in the surface layer, triggered by the electron-induced desorption of anions. Similar surface modifications are sometimes observed in the MgO films after spectral acquisition. The importance of such desorption processes for the optical characteristics is not clear at this moment and will be explored in future electro-luminescence experiments performed at smaller excitation energy.

4. Conclusion

Flat and defect-poor MgO films have been grown on a Mo(001) support, as revealed by STM and LEED measurements. The film morphology depends critically on the number of MgO layers and passes through different stages with increasing thickness, such as a coincidence lattice with the Mo support and a dislocation network. Optical properties of MgO films are dominated by two emission bands located at 3.1 and 4.4 eV, which have tentatively been assigned to the radiative decay of MgO excitons at 3-fold and 4-fold coordinated sites. The local nature of the employed technique, namely stimulating light emission by electron injection from an STM tip, will hopefully lead to an atomic-scale correlation between well-defined MgO surface features and distinct optical emission bands in future.

Acknowledgement

We are indebted to Dr. M. Sterrer for many experimental suggestions and helpful discussions.

References

[1] G. Ertl, H. Knözinger, J. Weitkamp (Eds.), Handbook of Heterogenous Catalysis, vol. 4, Wiley–VCH, Weinheim, 1997, p. 2111.
[2] M. Bäumer, H.-J. Freund, Prog. Surf. Sci. 61 (1999) 127.
[3] P. Luches, S. Benedetti, M. Liberati, F. Boscherini, I.I. Pronin, S. Valeri, Surf. Sci. 583 (2005) 191.
[4] M.C. Wu, J.S. Corneille, C.A. Estrada, J.W. He, D.W. Goodman, Chem. Phys. Lett. 182 (1991) 472.
[5] J. Wollschläger, J. Viernow, C. Tegenkamp, D. Erdös, K.M. Schröder, H. Pfnür, Appl. Surf. Sci. 142 (1999) 129.
[6] S. Valeri, S. Altieri, A. di Bona, C. Giovanardi, T.S. Moia, Thin Solid Films 400 (2001) 16.
[7] S. Valeri, S. Altieri, A. di Bona, P. Luches, C. Giovanardi, T.S. Moia, Surf. Sci. 507–510 (2002) 311.
[8] S. Schintke et al., Phys. Rev. Lett. 87 (2001) 276801.
[9] M. Sterrer et al., J. Phys. Chem. B 110 (2006) 46.
[10] H.L. Meyerheim et al., Phys. Rev. Lett. 87 (2001) 076102.
[11] M. Klaua et al., Phys. Rev. B 64 (2001) 134411.
[12] J.S. Corneille, J.W. He, D.W. Goodman, Surf. Sci. 306 (1994) 269.
[13] M. Sterrer, E. Fischbach, T. Risse, H.-J. Freund, Phys. Rev. Lett. 94 (2005) 186101.
[14] M.C. Gallagher, M.S. Fyfield, L.A. Bumm, J.P. Cowin, S.A. Joyce, Thin Solid Films 445 (2003) 90.
[15] R. Hacquart, J.M. Krafft, G. Costentin, J. Jupille, Surf. Sci. 595 (2005) 172.
[16] M.L. Bailly, G. Costentin, H.L. Pernot, J.M. Krafft, M. Che, J. Phys. Chem. B 109 (2005) 2404.
[17] S. Stankic, M. Muller, O. Diwald, M. Sterrer, E. Knözinger, J. Bernardi, Angew. Chem., Int. Ed. 44 (2005) 4917.
[18] S. Coluccia, A.M. Deane, A.J. Tench, J. Chem. Soc., Faraday Trans. 1 (74) (1978) 2913.
[19] M. Anpo, Y. Yamada, Y. Kubokawa, S. Coluccia, A. Zecchina, M. Che, J. Chem. Soc., Faraday Trans. 1 (84) (1988) 751.
[20] N. Nilius, N. Ernst, H.-J. Freund, Phys. Rev. Lett. 84 (2000) 3994.
[21] J. Wollschläger, D. Erdös, H. Goldbach, R. Höpken, K.M. Schröder, Thin Solid Films 400 (2001) 1.
[22] M. Dynna, J.L. Vassent, A. Marty, J. Appl. Phys. 80 (1996) 2650.
[23] A.M. Ferrari, S. Casassa, C. Pisani, S. Altieri, A. Rota, S. Valeri, Surf. Sci. 588 (2005) 160.
[24] E.D.L. Rienks, N. Nilius, H.-P. Rust, H.-J. Freund, Phys. Rev. B 71 (2005) 241404.
[25] H. Brune, M. Giovannini, K. Bromann, K. Kern, Nature 394 (1998) 451.
[26] (a) A.L. Shluger, P.V. Sushko, L.N. Kantorovich, Phys. Rev. B 59 (1999) 2417;
(b) P.V. Sushko, J.L. Gavartin, A.L. Shluger, J. Phys. Chem. B 106 (2002) 2269.
[27] P.V. Sushko, A.L. Shluger, C. Catlow, Surf. Sci. 450 (2000) 153.
[28] G.H. Rosenblatt, M.W. Rowe, G.P. Williams Jr., R.T. Williams, Y. Chen, Phys. Rev. B 39 (1989) 10309.
[29] J. Kramer, W. Ernst, C. Tegenkamp, H. Pfnür, Surf. Sci. 517 (2002) 87.
[30] B. Such, P. Czuba, P. Piatkowski, M. Szymonski, Surf. Sci. 451 (2000) 203.
[31] J. Wollschläger et al., Appl. Surf. Sci. 162 (2000) 309.
[32] W.P. Hess, A.G. Joly, K.M. Beck, M. Henyk, P.V. Sushko, P.E. Trevisanutto, A.L. Shluger, J. Phys. Chem. B 109 (2005) 19563.